Wavelet treatment of the intrachain correlation functions of homopolymers in dilute solutions

M. V. Fedorov*
Theory and Computation Group, Centre for Synthesis and Chemical Biology, Conway Institute of Biomolecular and Biomedical Research, Department of Chemistry, University College Dublin, Belfield, Dublin 4, Ireland

G. N. Chuev†
Institute of Theoretical and Experimental Biophysics, Russian Academy of Sciences, Pushchino, Moscow Region, 142290, Russia

Yu. A. Kuznetsov‡
Computing Centre, University College Dublin, Belfield, Dublin 4, Ireland

E. G. Timoshenko§
Theory and Computation Group, Centre for Synthesis and Chemical Biology, Conway Institute of Biomolecular and Biomedical Research, Department of Chemistry, University College Dublin, Belfield, Dublin 4, Ireland
(Received 11 June 2004; revised manuscript received 21 September 2004; published 15 November 2004)

Discrete wavelets are applied to the parametrization of the intrachain two-point correlation functions of homopolymers in dilute solutions obtained from Monte Carlo simulations. Several orthogonal and biorthogonal basis sets have been investigated for use in the truncated wavelet approximation. The quality of the approximation has been assessed by calculation of the scaling exponents obtained from the des Cloizeaux ansatz for the correlation functions of homopolymers with different connectivities in a good solvent. The resulting exponents are in better agreement with those from recent renormalization group calculations as compared to the data without the wavelet denoising. We also discuss how the wavelet treatment improves the quality of data for correlation functions from simulations of homopolymers at varied solvent conditions and of heteropolymers.

DOI: 10.1103/PhysRevE.70.051803 PACS number(s): 61.25.Hq, 02.60.−x, 36.20.Ey

I. INTRODUCTION

The main purpose of this paper is to give a useful introduction and practical guide to those who would like to apply discrete wavelets for treating the data for the intrachain two-point correlation functions (TPCF's) $g_{ij}^{(2)}(r)$, which either have been previously computed from direct computer simulations, came from some theoretical technique after solving equations for TPCF's, or perhaps have been obtained from x-ray and neutron scattering experiments. The intrachain correlation functions represent a fundamental link between the equilibrium thermodynamic observables and the conformational structure of polymers. These functions for polymers exhibit rather different behavior depending on the solvent quality. The TPCF of a homopolymer in a good solvent follows a universal scaling scaling law[1] for which analytical expressions can be derived by the field theoretical and other approaches [1–3]. On the contrary, the TPCF's in a poor solvent exhibit a complicated oscillating radial dependence akin to that of simple liquids. In this case, there is no known simply parametrized representation of TPCF's for the homopolymer globule. Moreover, an accurate sampling around a rather tall peak corresponding to the first solvation shell becomes very significant as this peak contributes most to the thermodynamic observables such as the mean energy. On the other hand, TPCF's in a good solvent obtained from molecular mechanics simulations tend to be rather noisy due to the high entropy of the coil conformation. This results in a large scatter of values of TPCF's at small radial separations, which makes further fitting of the data by an analytical expression and extraction of the scaling exponents difficult. Therefore, in general, dealing with the TPCF data of heteropolymers, for which some monomers are in a good solvent while others are in a poor solvent, and, particularly, extracting meaningful information from such data is a rather nontrivial problem.

Relying on the recent works of some of us [4–6], we believe that the task of parametrizing $g_{ij}^{(2)}(r)$ in a compact way can be accomplished by means of the multiresolution analysis [7,8]. At present, a number of special basis sets, referred to as wavelets [9], are known and are being actively used for treating both smooth and sharply oscillating functions, as well as for denoising of signals [10,11]. Wavelets have become a necessary mathematical tool in many modern theoretical investigations in physics, chemistry, and other fields [12–22]. Wavelets are particularly useful in those cases when the result of the analysis of a function should contain not only the list of its typical frequencies (scales), but also

*Electronic address: Maxim.Fedorov@ucd.ie
†Electronic address: genchuev@rambler.ru
‡Electronic address: Yuri.Kuznetsov@ucd.ie
§Author to whom correspondence should be addressed.
Electronic address: Edward.Timoshenko@ucd.ie
URL: http://darkstar.ucd.ie

[1]Strictly speaking [28], such laws are asymptotic in nature and do not apply when the two monomers are too close to each other in terms of the connectivity or when the interaction parameters are far from the the appropriate fixed point.

the list of the local coordinates where these frequencies are important. Thus, the main field of applications of wavelets is to analyze and process different classes of functions which are either nonstationary (in time) or inhomogeneous (in space).

The most general principle of the wavelet construction is to use dilations and translations. Commonly used wavelets form a complete (bi)orthonormal system of functions with a finite support constructed in such a way. That is why by changing a scale (dilations) wavelets can distinguish the local characteristics of a function at various scales and by translations they cover the whole region in which a function is being studied. Due to the completeness of the base system, wavelets also allow one to perform the inverse transformation to decomposition, which is called reconstruction.

In the analysis of functions with a complicated behavior, the locality property of wavelets makes the wavelet transform technique substantially advantageous compared to the Fourier transform. The latter provides one only with the knowledge of global frequencies (scales) of a function under investigation since the system of the base functions used (sine, cosine, or imaginary exponential functions) is defined on the infinite range. The special features of wavelets such as their (bi)orthogonality and vanishing of moments result in the need for only a few approximating coefficients in practical applications. That is a reason why wavelets are actively used, for example, to construct distribution functions in calculations of the electronic structure [19–21] as well as in statistical mechanics [4–6].

Recently, some of us have carried out several studies devoted to the wavelet parametrization of the radial density functions for various atomic and molecular solutes [4–6]. A model study of the galaxies density in Ref. [22] uses a similar wavelet approach for a different problem. In the present work we would like to address the question whether wavelets can also be advantageous for approximating the intrachain correlation functions of homopolymers in different solvents. The main practical goal of this paper is to apply discrete wavelets for approximating functions $g_{ij}^{(2)}(r)$ of open, ring, and star homopolymers in a coil conformation, as well as of a globule. In the case of a coil, the des Cloizeaux scaling formula applies and a number of accurate theoretical results for the scaling exponents involved are available [1,23]. Thus, we shall be able to investigate the influence of the choice of the wavelet basis set and of the number of terms not only on the quality of the correlation function parametrization, but also on the values of the scaling exponents extracted from fitting the wavelet denoised functions by the des Cloizeaux formula.

II. METHODS

A. Model

To obtain the correlation functions we relied on the standard coarse-grained homopolymer model [24–26] based on the following Hamiltonian in terms of the monomer coordinates, $\mathbf{X}_i$:

$$H = \frac{k_B T}{2\ell^2} \sum_{i\sim j} k_{ij} (\mathbf{X}_i - \mathbf{X}_j)^2 + \frac{1}{2} \sum_{ij,\ i\neq j} V(|\mathbf{X}_i - \mathbf{X}_j|). \quad (1)$$

The first term here represents the connectivity structure of the polymer with harmonic springs of a given strength κ_{ij} introduced between any pair of connected monomers (denoted by $i\sim j$). The second term represents pairwise nonbonded interactions between monomers such as the van der Waals forces, for which we adopt the Lennard-Jones form of the potential,

$$V(r) = \begin{cases} +\infty, & r < d, \\ V_0 \left[\left(\frac{d}{r}\right)^{12} - \left(\frac{d}{r}\right)^{6} \right], & r > d, \end{cases} \quad (2)$$

where there is also a hard-core part with monomer diameter d (below we choose $d=\ell$ without any lack of generality).

We use the Monte Carlo technique with the standard Metropolis algorithm [27], which converges to the Gibbs equilibrium ensemble, based upon the implementation described by us in [25]. The value of $V_0=0$ will correspond to the purely repulsive case (good solvent) leading to a coil conformation of the polymer, while $V_0=5\ k_BT$ will correspond to the attractive case (poor solvent) leading to a globular conformation as in Ref. [28]. All details of our Monte Carlo procedure have been previously described in Ref. [28] and, in fact, here we shall rely on the same set of Monte Carlo simulation data in order to make the comparison of the wavelet treated scaling exponents with those of Ref. [28] more straightforward and unambiguous.

B. Correlation functions

The intrachain two-point correlation function of a pair of monomers i and j is defined as

$$g_{ij}^{(2)}(\mathbf{r}) \equiv \langle \delta(\mathbf{X}_i - \mathbf{X}_j - \mathbf{r}) \rangle = \frac{1}{4\pi r^2} \langle \delta(|\mathbf{X}_i - \mathbf{X}_j| - r) \rangle. \quad (3)$$

The second equation establishes that it is a function of radius $r=|\mathbf{r}|$ only due to spatial isotropy [SO(3) rotational symmetry]. We may note that this function should, strictly speaking, be named a distribution function, but since $g_{ij}^{(2)}(r)\to 0$ when $r\to\infty$ because of the chain connectivity, we apply the term "correlation function" to $g_{ij}^{(2)}(r)$ itself rather than to the quantity $g_{ij}^{(2)}(r)/(g^{(1)})^2-1$, which would vanish as $r\to\infty$ in the case of simple liquids. The function is normalized to unity via $\int d^3\mathbf{r} g_{ij}^{(2)}(\mathbf{r})=1$. Note that the correlation functions exactly satisfy the excluded volume condition, $g_{ij}^{(2)}(r)=0$ for $r<d$, due to the choice of hard-core part in the nonbonded potential Eq. (2). The mean-squared distance between monomers i and j is

$$D_{ij} \equiv \left\langle (\mathbf{X}_i - \mathbf{X}_j)^2 \right\rangle = \int d^3\mathbf{r} |\mathbf{r}|^2 g_{ij}^{(2)}(\mathbf{r}), \quad (4)$$

which we defined here without the traditional factor of $1/3$ as compared to some of the previous papers [25].

The intrachain pair correlation functions $g_{ij}^{(2)}(r)$ are strongly dependent on both the degree of polymerization K

of the polymer and the choice of the reference monomers i and j, contacts between which we are looking at. However, as we have demonstrated in Ref. [28], if we introduce the rescaled correlation function in terms of the dimensionless variables,

$$\hat{g}_{ij}^{(2)}(\hat{r}) \equiv D_{ij}^{3/2} g_{ij}^{(2)}(r), \quad \hat{r} \equiv r/D_{ij}^{1/2}, \tag{5}$$

these will change in about the same range and hence would permit a much more straightforward comparison with each other. From this definition, obviously, $\hat{g}_{ij}^{(2)}(\hat{r})$ satisfies the following two normalization conditions:

$$\int_0^\infty d\hat{r}\hat{r}^2 \hat{g}_{ij}^{(2)}(\hat{r}) = \int_0^\infty d\hat{r}\hat{r}^4 \hat{g}_{ij}^{(2)}(\hat{r}) = \frac{1}{4\pi}. \tag{6}$$

C. Scaling relations

According to Refs. [1,3] TPCF's of a flexible homopolymer coil in a good solvent can be well described [28] via a power law times a stretched exponential, known as the des Cloizeaux scaling equation:

$$\hat{g}_{ij}^{(2)}(\hat{r}) = A_{ij}\hat{r}^{\theta_{ij}} \exp(-B_{ij}\hat{r}^{\delta_{ij}}). \tag{7}$$

Due to the two normalization conditions in Eq. (6), the constants A and B can be immediately calculated and expressed via θ and δ. The exponents δ_{ij} do not really depend on i, j, but the contact exponents θ_{ij} do. In the case of the end-end correlations of an open chain θ_{ij} is denoted as θ_0, and these can be expressed via

$$\delta = \frac{1}{1-\nu}, \quad \theta_0 = \frac{\gamma - 1}{\nu}, \tag{8}$$

where ν has the meaning of the inverse fractal dimension of the system and γ is related to the number of different polymer conformations [1,3].

D. Wavelet theory

The fundamental theory behind wavelets is known as the multiresolution analysis (MRA). Most of the rigorous results and definitions from MRA are not usually required for practical applications. The only equations which are needed for the work described herein will be introduced in this section. As we mainly use basis sets from the biorthogonal wavelets families, we shall introduce all wavelets in a general way as biorthogonal wavelets. Moreover, we shall use the discrete wavelet transform (DWT) technique [7,9] to parametrize the TPCF's. There is a good introduction to the wavelet techniques in Ref. [15]. We also will follow the style of that book henceforth. The multiresolution approach is based on the idea that the wavelet functions generate a hierarchical sequence of subspaces in the space of square-integrable functions over the real axis $L^2(\mathbb{R})$, which forms the MRA.

The scaling functions $\varphi(r)$ and $\tilde{\varphi}(r)$ produce a biorthogonal MRA if they satisfy the following conditions.

(i) Translations of these functions with integers $\varphi_s = \varphi(r-s)$, $\tilde{\varphi}_s = \tilde{\varphi}(r-s)$, $s \in \mathbb{Z}$, are linearly independent and produce bases of the subspace $V_0 \subset L^2(\mathbb{R})$ and their dual counterpart $\tilde{V}_0 \subset L^2(\mathbb{R})$ correspondingly. This means that if a function $f(r)$ is contained in the space V_j, its integer translations have to be contained in the same space:

$$f(r) \in V_j \Leftrightarrow f(r+s) \in V_j,$$
$$f(r) \in \tilde{V}_j \Leftrightarrow f(r+s) \in \tilde{V}_j, \quad s \in \mathbb{Z}.$$

(ii) Dyadic dilates of these functions $\varphi_{js} = \varphi(2^j r - s)$, $\tilde{\varphi}_{js} = \tilde{\varphi}(2^j r - s)$, $j \in \mathbb{Z}$, generate hierarchical sets of subspaces $\{V_j\}$ and $\{\tilde{V}_j\}$, so that

$$V_j \subset V_{j+1}, \quad \bigcup_{j=-\infty}^{\infty} V_j \text{ is dense in } L^2(\mathbb{R}), \quad \bigcap_{j=-\infty}^{\infty} V_j = 0,$$

$$\tilde{V}_j \subset \tilde{V}_{j+1}, \quad \bigcup_{j=-\infty}^{\infty} \tilde{V}_j \text{ is dense in } L^2(\mathbb{R}), \quad \bigcap_{j=-\infty}^{\infty} \tilde{V}_j = 0. \tag{9}$$

(iii) The sets of functions $\varphi_{js}(r)$ and $\tilde{\varphi}_{js}(r)$ are biorthogonal to each other. It means that for any s, $s' \in \mathbb{Z}$:

$$\int \varphi_{js}(r)\tilde{\varphi}_{js'}(r)dr = \delta_{ss'}.$$

It means that if a function $f(r)$ is contained in the space V_j, the compressed function $f(2r)$ has to be contained in the higher-resolution space V_{j+1}:

$$f(r) \in V_j \Leftrightarrow f(2r) \in V_{j+1},$$

$$f(r) \in \tilde{V}_j \Leftrightarrow f(2r) \in \tilde{V}_{j+1}, \quad j \in \mathbb{Z}.$$

(iv) There is a wavelet function $\psi(r)$ and its dual wavelet function $\tilde{\psi}(r)$ such that their integer translations $\psi_s(r) = \psi(r-s)$, $\tilde{\psi}_s(r) = \tilde{\psi}(r-s)$ and dyadic dilates $\psi_{js} = \psi(2^j r - s)$, $\tilde{\psi}_{js} = \tilde{\psi}(2^j r - s)$ form subspaces W_j and $\tilde{W}_j$ which are complementary to V_j and $\tilde{V}_j$ so that

$$V_{j+1} = V_j \oplus W_j, \quad \tilde{V}_{j+1} = \tilde{V}_j \oplus \tilde{W}_j, \quad \tilde{W}_j \perp V_j, \quad \tilde{V}_j \perp W_j. \tag{10}$$

(v) From the above relations it follows that $L^2(\mathbb{R})$ can be decomposed into the approximation space V_{j_0} and the sum of the detailed spaces W_j of higher resolutions $j \geqslant j_0$:

$$L^2(\mathbb{R}) = V_{j_0} \oplus \bigoplus_{j \geqslant j_0}^{\infty} W_j, \tag{11}$$

where $j_0 \in \mathbb{Z}$ is a chosen level of resolution. This means that any square-integrable function $f(r)$ can be represented as a sum of linear combinations of the reconstruction scaling functions $\{\varphi_{j_0}\}$ at a chosen resolution $j = j_0$ and the reconstruction wavelet functions $\{\psi_j\}$ at all finer resolutions $j \geqslant j_0$. This can be written as

$$f(r) = \sum_s a_{j_0 s}\varphi_{j_0 s}(r) + \sum_{j>j_0}^{\infty}\sum_s d_{js}\psi_{js}(r), \tag{12}$$

where the coefficients $\{a_{j_0 s}\}$ and $\{d_{js}\}$ are obtained as the scalar products with the appropriate dual decomposition basis functions

$$a_{js} = \int f(r)\tilde{\varphi}_{js}(r)dr, \quad d_{js} = \int f(r)\tilde{\psi}_{js}(r)dr. \tag{13}$$

The later equation defines the discrete wavelet transform.

As $\varphi(r) \subset V_0$ and $V_0 \subset V_1$, $\tilde{\varphi}(r) \subset \tilde{V}_0$ and $\tilde{V}_0 \subset \tilde{V}_1$, we can express $\varphi(r)$ [as well as $\tilde{\varphi}(r)$] as a linear combination of the basis functions in $V_1[\tilde{V}_1]$:

$$\varphi(r) = \sum_s h_s \varphi(2r-s), \quad \tilde{\varphi}(r) = \sum_s \tilde{h}_s \tilde{\varphi}(2r-s). \tag{14}$$

This equation is called the *dilation equation*. Similarly, $\psi(r)$ and $\tilde{\psi}(r)$ must satisfy a *wavelet dilation equation*:

$$\psi(r) = \sum_s w_s \varphi(2r-s), \quad \tilde{\psi}(r) = \sum_s \tilde{w}_s \tilde{\varphi}(2r-s). \tag{15}$$

The above sets of coefficients are usually called "filters" and they are completely sufficient in order to describe a chosen wavelet basis because there are several procedures on how to build up numerical values of the wavelet functions from the set of filters [7,9,15]. We should emphasize here that there are no analytic expressions for biorthogonal (orthogonal) wavelets with a finite support[2] These are determined in terms of their filter coefficients only. But one can obtain the values of these functions with any given accuracy by using special procedures, which are well described in the wavelet literature [7,9,15].

The scaling functions and the wavelets have a finite support only in the case of a finite number of the coefficients h_s and w_s. Due to their biorthogonal nature, these functions satisfy the relations

$$\begin{aligned}
&\int \varphi_{ja}(r)\tilde{\varphi}_{jb}(r)\,dr = \delta_{ab},\\
&\int \varphi_{ja}(r)\tilde{\psi}_{lb}(r)\,dr = 0 \quad (l \geqslant j),\\
&\int \tilde{\varphi}_{ja}(r)\psi_{lb}(r)\,dr = 0 \quad (j \geqslant l),\\
&\int \psi_{ja}(r)\tilde{\psi}_{kb}(r)\,dr = \delta_{jk}\delta_{ab},
\end{aligned} \tag{16}$$

for any integer j, l, a, b.

If the pairs of the decomposition functions $\{\tilde{\varphi}, \tilde{\psi}\}$ and the reconstruction functions $\{\varphi, \psi\}$ are identical, the transform is called the "orthogonal wavelet transform." Otherwise we shall talk about a more general "biorthogonal wavelet transform."

In the expansion (12) the first term gives a "coarse" approximation for $f(r)$ at the resolution j_0 and the second term gives a sequence of successive "details." In practice, we actually do not need to use an infinite number of resolutions. Therefore, the sequence of details is cut off at an appropriate resolution $j_{\max}$. Since all functions used in numerical work are given in a finite interval, the sequence of different translations $\{s\}$ has also a finite number of terms, S. It should be mentioned that, really, S can be different for detailed and coarse approximations.

Importantly, the explicit form of the basis functions is not required if we are using (bi)orthogonal wavelets with a finite support and a dyadic set of scales j. Then the coefficients in Eq. (13) can be calculated by the fast wavelet transform (FWT) algorithm [7,8,15]. The main idea of this algorithm is that a set of (bi)orthogonal discrete filters at consequently dilated scales is used for the multiresolution analysis of a signal. As a result, to calculate the approximating coefficients, the convolution of the signal and the relevant filter is only required for each scale, and the latter can be easily obtained.

By choosing relevant basis functions and scales we can nullify most of the coefficients $\{a\}$ and $\{d\}$ thereby reducing the square root error (SRE) since the DWT satisfies Parseval's identity [9]. Therefore, the function under study can be reconstructed with the use of only a few nonzero coefficients without any significant loss of accuracy, making the total number of approximating coefficients rather small. This feature of the of wavelet approximation is widely used in the processing of signals and images, the data for which should be compressed with minimal losses [10].

E. Choice of wavelet basis set

The compression and denoising properties of the wavelet transform strongly depended on the fundamental properties of the wavelet bases, which we define here in a rather simplified way as the *number of vanishing moments, regularity, size of support, symmetry, and orthogonality and biorthogonality*.

Number of vanishing moments. A wavelet function $\psi(r)$ has N_{VM} vanishing moments (VM) if

$$\int r^{\mu}\psi(r)dr = 0 \quad \text{for} \quad \mu = 0,\ldots,N_{\mathrm{VM}}-1. \tag{17}$$

The number of vanishing moments strongly influences the localization of wavelets in the frequency space. The Fourier transform of a wavelet with $N_{\mathrm{VM}}=n$ has a peak and decays as k^{-n} (k means frequency).

Regularity. This can be defined as the number ρ of existing derivatives of a wavelet function. It also characterizes the frequency localization of wavelets. The Fourier transform of a wavelet with regularity $\rho=n$ decays as $k^{-(n+1)}$ for large k. We would like to emphasize that as wavelets have no analytic expressions the definition of their derivatives is not as straightforward as for the "usual" functions [9]. However,

[2]This is true except of the simplest basis, Haar basis, which is constructed from piecewise functions [9].

these mathematical details are beyond the scope of our article.

Size of support. This is the length of the interval on which the wavelet function has nonzero values. Obviously, this characterizes the space localization of the wavelet.

Symmetry. The wavelet bases functions can be strongly symmetric or asymmetric. The deviation of a wavelet from the symmetry (i.e., even or odd parity) is usually measured by how the phase of its Fourier transform deviates from a linear function. It was shown that is impossible to construct an orthogonal basis with the exact parity of the functions.[3]

On the contrary, we can design a biorthogonal basis set with the exact symmetry of the function without serious efforts [9,29].

Orthogonality and biorthogonality. As we have already mentioned in the case when the pairs of the decomposition functions $\{\tilde{\varphi}, \tilde{\psi}\}$ and the reconstruction functions $\{\varphi, \psi\}$ are identical, the wavelet transform is orthogonal. Otherwise it is biorthogonal. But this is true only if the $\{\tilde{\varphi}, \tilde{\psi}\}$ and $\{\varphi, \psi\}$ obey the conditions (16). We should mention that there are several nonorthogonal families of wavelets such as Mexican hat, Morle, Gaussian wavelets, and so on [8,9,11]. Usually they have infinite support and do not obey exactly Parseval's identity. Therefore such wavelets do not provide a one-to-one reconstruction of a function from the its wavelet expansion coefficients. Due to these circumstances, we do not use such basis sets in our work.

Summing up the above, we can conclude that in order to provide good denoising of a signal the wavelets have to possess good regularity and as many vanishing moments as possible. From another point of view, they have to be well localized in space, which means that they must have a quite short support. Unfortunately, these properties are interrelated. Thus, a small support implies only a few vanishing moments and poor regularity. In addition, the orthogonality implies asymmetry of the basis functions, which in turn can lead to some numerical artifacts. Since for each concrete task certain wavelet properties are more important than others, there are different wavelet families which are optimized for some of these properties.

For example, in the case of Daubechies wavelets we have a maximum number of vanishing moments and maximal asymmetry with fixed length of support, while the Symlet wavelet family has the "least asymmetry" and highest number of vanishing moments with a given support width.

It was shown that it is possible to construct wavelet basis sets with the scaling function having vanishing moments of nonzero order with respect to some shifting constant c. Thus, for a given number of vanishing moments, N_{VM}, we have

$$\int (r-c)^n \psi(r) dr = 0, \quad 0 < n < N_{\mathrm{VM}}.$$

The Coifman wavelets are compactly supported wavelets which have the highest number of vanishing moments for both $\varphi(r)$ and $\psi(r)$ with a given width of support. This property is very useful for the treatment of functions with sharp peaks and slopes. The larger the number of scaling function vanishing moments, the better is the approximation for singular points of the function under study [9]. Hence, by using such wavelets (e.g., Coifman) we can treat accurately sharp peaks of such a function. On the other hand, these wavelets are rather smooth to approximate well the function within the ranges between these peaks. The price for this extra feature is that the Coifman wavelets are longer than the Daubechies wavelets. Their length of support is equal to $3N_{\mathrm{VM}}-1$ instead of $2N_{\mathrm{VM}}-1$.

Thus we can see that for orthogonal wavelets the desirable properties are in contradiction with each other. But fortunately, we can use different functions for the decomposition and reconstruction. These biorthogonal bases have several advantages compared with the orthogonal bases. We can also benefit from the fact that we can use the base functions $\tilde{\varphi}$, $\tilde{\psi}$ with a number of vanishing moments for decomposition, whereas the functions φ, ψ with a good regularity for reconstruction. The former would separate any unpleasant stochastic oscillations of TPCF's leaving this "noise" to the detail coefficients at higher levels of resolution. The latter, on the other hand, would produce a TPCF approximation as smooth as possible during reconstruction. If, however, we would prefer to impose both conditions of a large number of vanishing moments and regularity on an orthogonal basis, we would have to pay with a support at least twice the size that of the biorthogonal basis. Large supports, on the other hand, are known to lead to a significant deterioration in the quality of the wavelet approximation [9,10].

In this work we will use biorthogonal bases from two biorthogonal families: biorthogonal spline wavelets whose decomposition functions $\tilde{\psi}(r)$ are optimized for the number of vanishing moments, but the reconstruction functions $\psi(r)$ are optimized in the sense of regularity; the reverse biorthogonal spline wavelets whose decomposition functions $\tilde{\psi}(r)$ are optimized to achieve maximal regularity with a given support width and the reconstruction functions $\psi(r)$ which are constructed in order to gain a maximum number of vanishing moments. In addition, these biorthogonal sets have the exact symmetry for all the basis functions.

F. Wavelet algorithm

A typical way of building the wavelet approximation is as follows [10]. The coefficients obtained by the FWT are sorted in the order of the decrease of their absolute values and then only some number L of the largest coefficients are kept by nullifying the rest of the coefficients. This is followed by application of the inverse transform (reconstruction). Note that the truncation number L depends on the required accuracy of representation of the function in question. However, this scheme is difficult to apply because of an undesired intersection between different levels of resolution which often arises. The latter leads to a much increased number of coefficients required without any sensible improvement in accuracy. The quality of the resulting approximation is not particularly high because the numerical boundary arti-

[3]The Haar basis is also an exception in this case.

facts result in the so-called Gibbs effect—i.e., false oscillations of the approximated function [9].

Therefore, we will use instead a "smarter" strategy in which we employ the following three remarkable circumstances.

(i) For physical reasons the functions $\hat{g}_{ij}^{(2)}(\hat{r})$ vanish at $\hat{r} \to 0$ (due to the excluded volume effect) and at $\hat{r} \to \infty$ (due to the finite size of the molecule).

(ii) In terms of the rescaled radius $\hat{r} \gtrsim 0.75$ the functions $\hat{g}_{ij}^{(2)}(\hat{r})$ have a rapid exponential (or even a faster stretched exponential) decay.

(iii) On physical grounds it is also well known that $gij(2)(r)$ is a differentiable function of a high order for large $\hat{r}$.

(iv) The multiresolution nature of the wavelet analysis allows us to treat each level of the wavelet decomposition separately.

We have developed an advanced scheme of the wavelet approximation which, first of all, takes into account the peculiarities of TPCF's. From another side it relies on the strategy of a "level-by-level" thresholding, which has been independently proposed by several authors [10,11].

By taking into account the asymptotic behavior of TPCF's, we can use the zero-boundary conditions while doing the wavelet decomposition. Considering the values of $\hat{g}(\hat{r} \to 0)$ as zero, we can also nullify all wavelet coefficients corresponding to the range [0,0.05]. Strictly speaking, the upper bound for this cutoff is given by $\hat{r}_l \equiv d/\sqrt{D_{ij}}$ and it depends on the system size and parameters, but the value of 0.05 is well below this bound for all data considered in this paper. As we have decomposition functions with a sufficient number of vanishing moments, we can nullify all detail coefficients at all levels of resolution which correspond to the range of rescaled radius $\hat{r} \in [0.75, \ldots, \infty)$ in order to extract the trends of our TPCF with a "maximal smoothness" [9,30]. The value for this lower bound $\hat{r}_r$ has the meaning of the rescaled radius after which the TPCF has a fairly smooth decaying behavior. For other regions of $\hat{r}$ we extract the *highest* detail coefficients in *each* level of resolution *separately*.

Summing up all of the above, we propose the following scheme for the TPCF wavelet approximation.

(i) We perform the FWT with zero-boundary conditions at the largest scale M satisfying the condition $\Sigma_b |d_{M,b}| \leqslant \epsilon \Sigma_b |a_{M,b}|$ (where a good choice for ϵ is 0.05); then, all further d coefficients can be neglected.

(ii) All the coefficients corresponding to the range $r \in [0, 0.05]$ (for both the approximation and detail) are also nullified.

(iii) We save *all* the approximation coefficients which remain nonvanishing in the previous steps.

(iv) All the *detail* coefficients corresponding to $r \in [0.75, \ldots, \infty)$ are nullified.

(v) In each level of decomposition we leave the maximal detail coefficients corresponding to the function extrema, while neglecting the rest of the coefficients.

(vi) We perform the conventional inverse FWT but only for the nonzero coefficients remaining from the previous steps.

(vii) To suppress the Gibbs effect at the left boundary, the approximated TPCF is set equal to zero up to r_{cross}, where r_{cross} is the rightmost nontrivial zero point of the approximated TPCF—i.e., $g_{app}(r_{cross}) = 0$.

As a result, we have a fast scheme of calculations and a compact approximation for the correlation functions.

Concerning the choice of the wavelet basis set, we note that to realize the FWT there are many suitable sets such as Daubechies, Coifman, Symlets, biorthogonal wavelets, and so on [9,29]. We have tested various basis sets, but our detailed study presented below indicates that the reverse biorthogonal basis (RB5-5) is the best of them for treatment of TPCF's for the systems under study. Here we shall follow the Daubechies notation for this family: the first index $N_d = 5$ for the decomposition functions, the second index $N_r = 5$ for the reconstruction ones. These indices reflect the number of vanishing moments of $\tilde{\psi}$—namely $N_{\mathrm{VM}} = N_r - 1$—the regularity value of ψ—namely, $\rho = N_r - 1$—as well as the length of support l for the pairs $\{\tilde{\varphi}, \tilde{\psi}\}$, $l_d = 2N_d + 1$, and for the pairs $\{\varphi, \psi\}$, $l_r = 2N_r + 1$. Figure 1 depicts the functions from the RB5-5 basis set.

III. RESULTS

To illustrate the usefulness of our scheme we have investigated the two-point correlation functions of ring, linear, and star homopolymers in the coil state, as well as of the globular state of a ring homopolymer since the connectivity is not as important for the latter state. The data for $\hat{g}_{ij}^{(2)}(\hat{r})$ have been obtained by the Monte Carlo simulations discussed in our previous study [28]. Figure 2 depicts the typical behavior of $\hat{g}_{ij}^{(2)}(\hat{r})$ for an open homopolymer coil and a ring homopolymer globule. As one can see, in the liquid globular state the TPCF has several peaks of increasing width and decreasing height located at approximately $nd/\sqrt{D_{ij}}$ $(n = 1, 2, \ldots)$. On the other hand, the TPCF of a coil exhibits a smoother radial dependence, but suffers from a significant statistical noise.

The correlation functions obtained from such data are then approximated by the above described wavelet procedure. Figure 3 shows the difference $\Delta\hat{g}(\hat{r}) = \hat{g}(\hat{r}) - \hat{g}_{app}(\hat{r})$ of the TPCF's obtained by simulations and their approximations by wavelets (solid curves) and cosines (dashed curves) with the same number of terms, L. One can clearly see that the wavelet treatment provides a much better approximation than the cosine Fourier treatment. For the coil $(L = 20)$, at small radial separations both treatments do show deviations from the simulation data, but these only reflect the limitations of sampling statistics of TPCF's as the function should really be very smooth and obey the des Cloizeaux equation. However, while the wavelet treatment gives an essentially vanishing $\Delta\hat{g}$ for larger $\hat{r}$, the Fourier treatment continues to yield parasitic oscillations at all separations. For the globule $(L = 25)$, which had a much better quality of data due to a smaller entropy of the globule, the wavelet treatment gives an essentially vanishing $\Delta\hat{g}$ everywhere, whereas the Fourier method works very poorly in the whole range with strong oscillations present even for the largest of separations.

In Fig. 4 we present four different levels of the wavelet decomposition of the TPCF of an open coil. We can see that

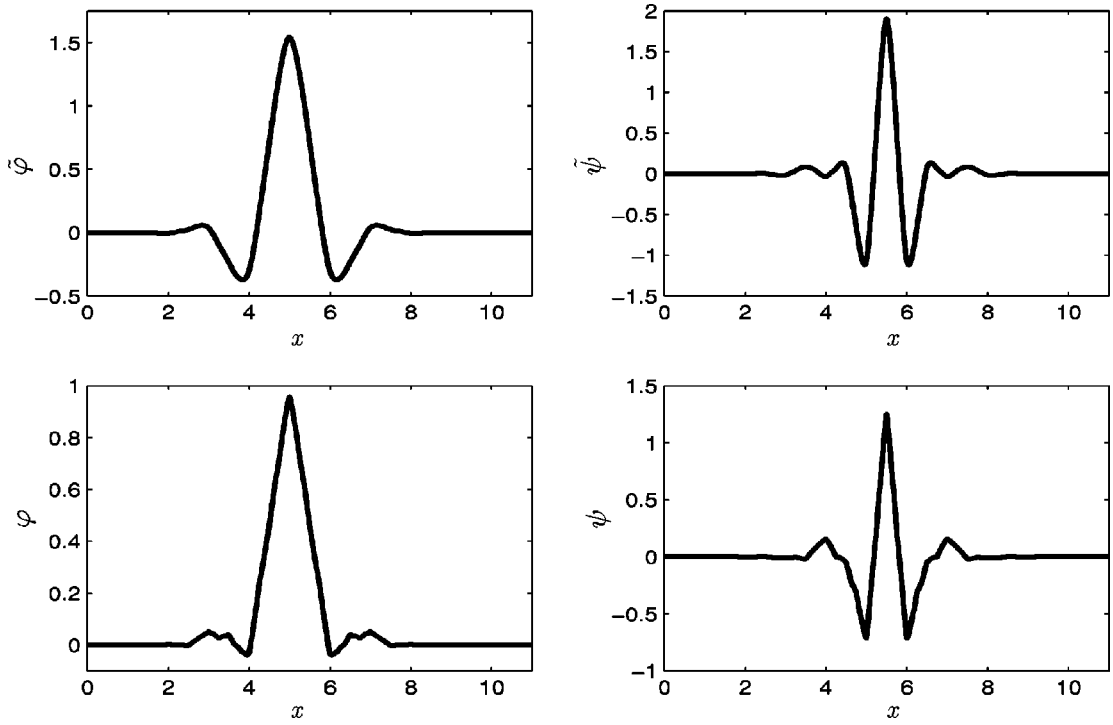

FIG. 1. Reverse biorthogonal spline wavelets 5-5. The abscissa is the real numbers axis ($x \in \mathbb{R}$). At the top are the decomposition scaling function $\tilde{\varphi}$ and the wavelet function $\tilde{\psi}$, and at the bottom are the corresponding reconstruction functions φ and ψ. Here and in all other figures the axes are depicted in dimensionless units.

the smooth part of this function can be well represented by the approximation coefficients. Conversely, the unpleasant oscillations are concentrated in the detail coefficients.

In Fig. 5 we likewise present four different levels of the wavelet decomposition of the TPCF for the globule of a ring homopolymer. We can see that the smooth part of this function can be mainly represented by the approximation coefficients. But there is also important information in the detail coefficients, which mainly represent the sharp peaks of the function. Therefore, our "smart" level-by-level technique allows us to effectively suppress noise in the case of the coil and to prevent us from "oversmoothing" of physical oscillations in case of the globule.

We have also calculated the mean-square norm of the inaccuracy Δ, which characterizes the quality of the approximation: $\Delta \equiv \sqrt{\Sigma_{i=1}^{n}[\hat{g}(\hat{r}_i)-\hat{g}_{app}(\hat{r}_i)]^2}$, where $\hat{r}_i = i\,\delta\hat{r}$ are the grid points, $\hat{g}(\hat{r}_i)$ is the "true" correlation function from Monte Carlo data, and $\hat{g}_{app}(\hat{r}_i)$ is the approximated one. Fig-

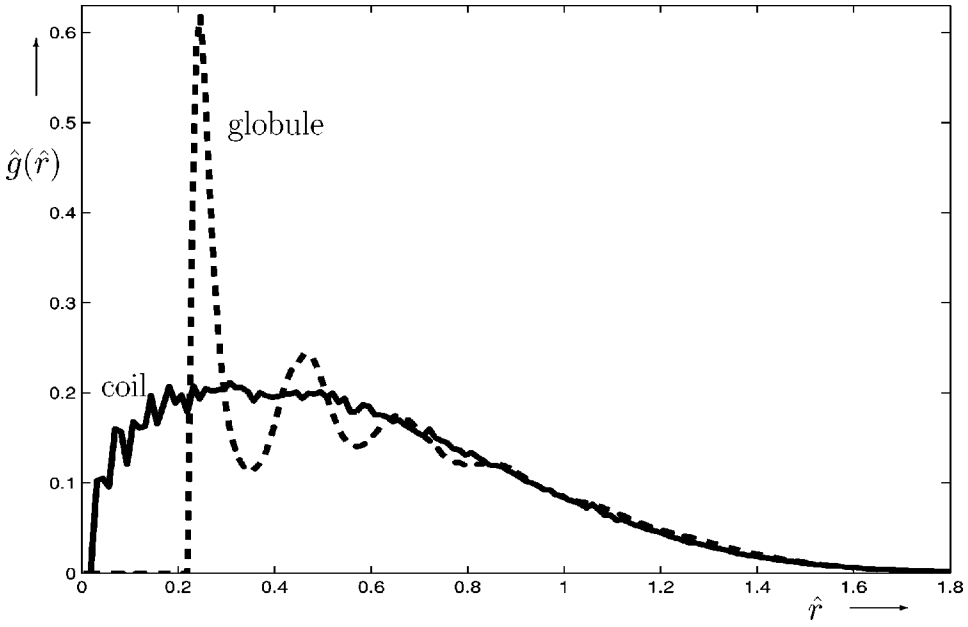

FIG. 2. Rescaled correlation function of the homopolymers with the degree of polymerization $K=200$. The solid curve corresponds to the end-end correlations of an open homopolymer in the coil state. The dashed curve corresponds to the globule of a ring homopolymer with $K=200$ and for $|i-j|=100$.

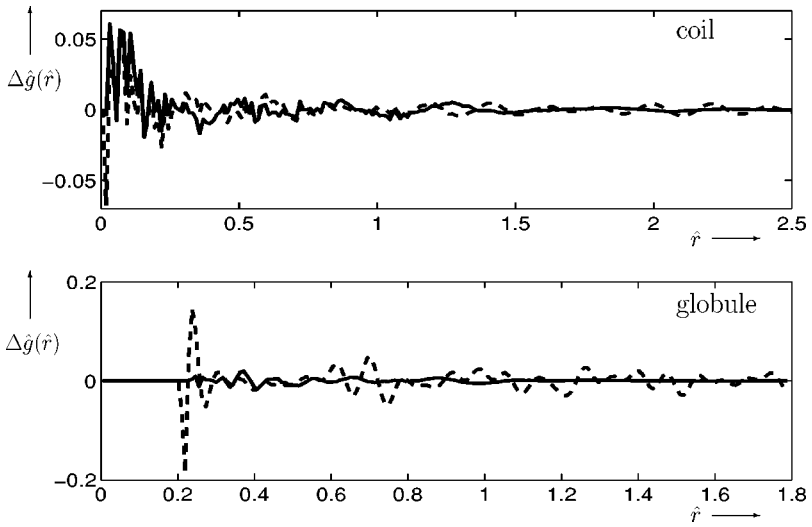

FIG. 3. The difference $\Delta\hat{g}(\hat{r})$ between the TPCF's obtained from simulations and their approximations by wavelets (solid curve) and cosines (dashed curve). The upper part of the figure corresponds to the coil of an open homopolymer, while the lower one to the globule of a ring homopolymer of the same lengths as in Fig. 2.

ures 6 and 7 depict the dependences of the norm Δ on the number L of approximating coefficients for the coil and globule states, respectively. In what was mentioned above we have used the "RB5-5" basis set [9]. Here, for comparison we also depict these dependences for the cosine and fast Fourier transform (FFT) approximation, which are widely used in applications [31]. We can see that for a reasonable number of coefficients the wavelet approximations give us a remarkably better accuracy than conventional methods.

For the approximated TPCF's we have also evaluated the scaling exponents for the coil state. In this case we can compare these results with the rather accurate theoretical values obtained from Borel-resumed renormalization group calculations [1,3,23,32]. As in Ref. [28] the fitting has been done via the the nonlinear least-squares (NLLS) Marquardt-Levenberg method [34] by means of the fit function in the gnuplot software. Fit reports parameter error estimates which are obtained from the variance-covariance matrix after the

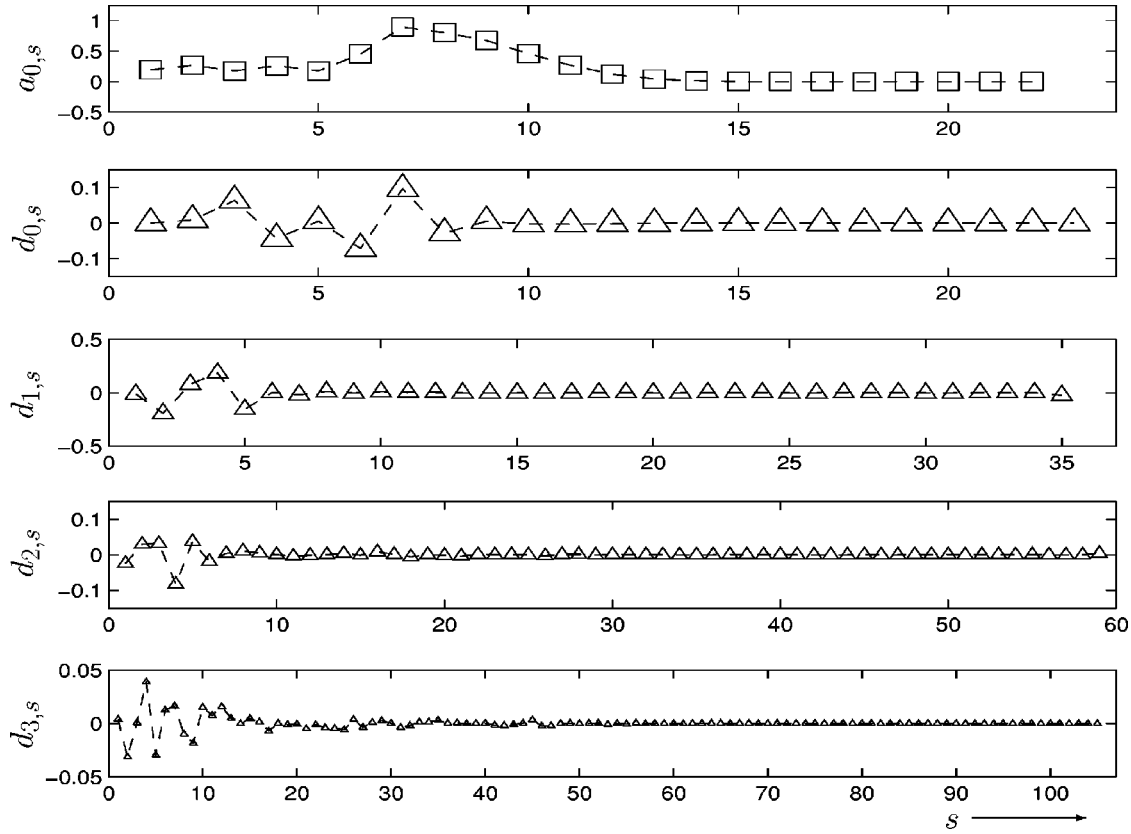

FIG. 4. Four different levels of the wavelet decomposition of the end-end TPCF of an open homopolymer with $K=200$. At the top there are approximating coefficients $\{a\}$ at the level $j_0=0$. The detail coefficients $\{d\}$ are presented in the ascending order in the level of the resolution j vs the shift parameter s.

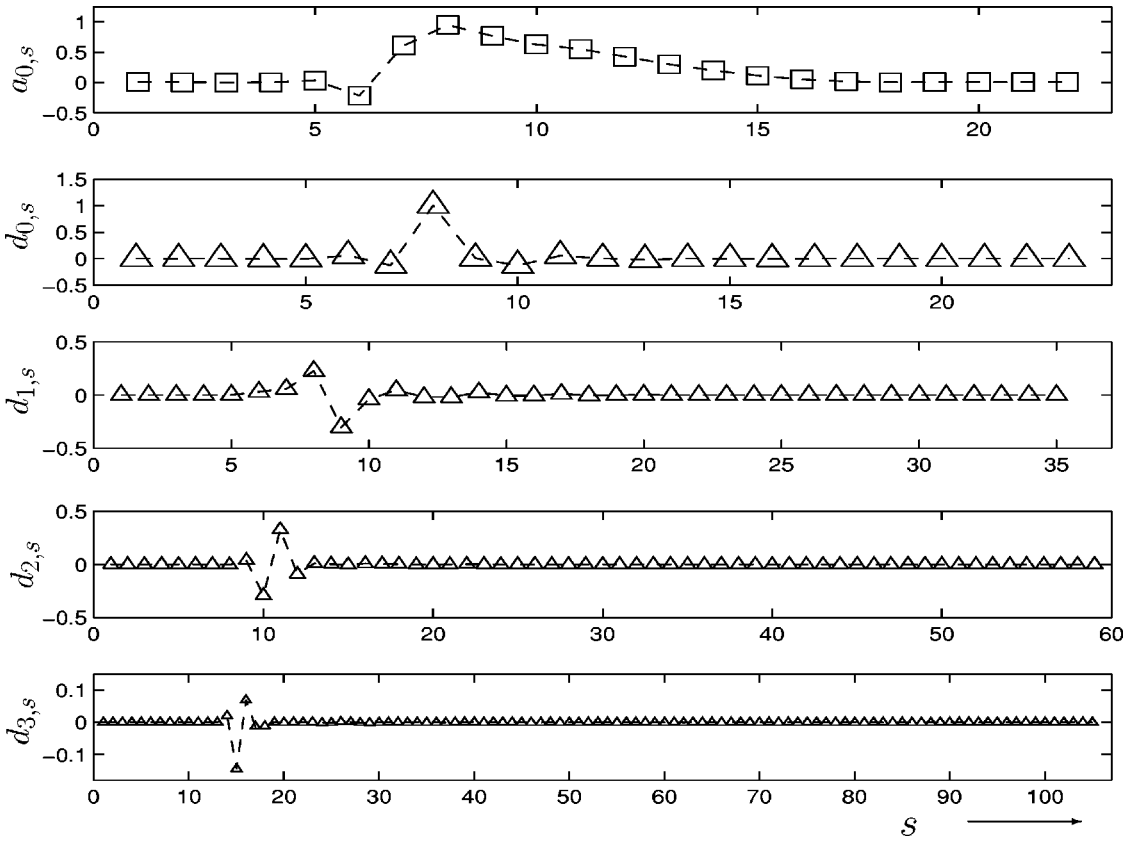

FIG. 5. Four different levels of the wavelet decomposition of the TPCF of the homopolymer globule of the same lengths and for the same chain indices as in Fig. 2. At the top there are approximating coefficients $\{a\}$ at the level $j_0=0$. The detail coefficients $\{d\}$ are presented in the ascending order in the level of the resolution j vs the shift parameter s.

final iteration. By convention, these estimates are called "standard errors" and they are reported in Table I, which contains the results for open and ring homopolymers. Here we have used the wavelet approximation with $L=20$ coefficients. In this table we also include the results which are obtained from the fitting of the untreated functions as in Ref. [28]. The notations in the first column follow the des Cloizeaux convention: 0, end-end monomers; 1, end-middle, $1'$, end-three-quarters; $1''$, end-one-quarter; and 2, one-quarter-three-quarters of the chain, respectively. Here and be-

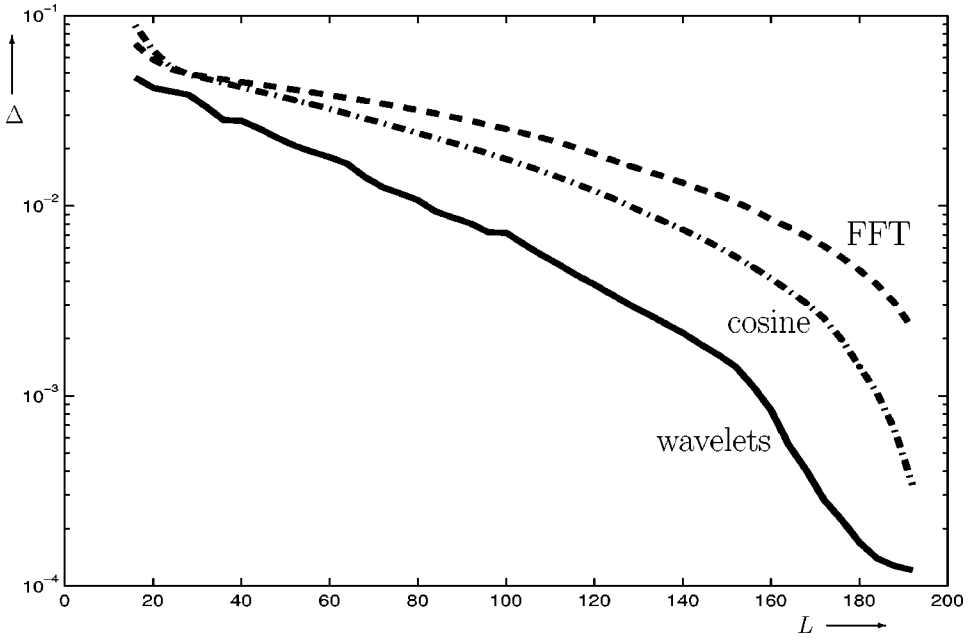

FIG. 6. Square-root error Δ between the rescaled end-end TPCF of a homopolymer ring in the coil state with the degree of polymerization $K=200$ and its approximations. The curves correspond to the wavelet approximation (solid line), FFT approximation (dashed line), and cosine approximation (dash-dotted line). The X axis is the total number L of the approximation coefficients used.

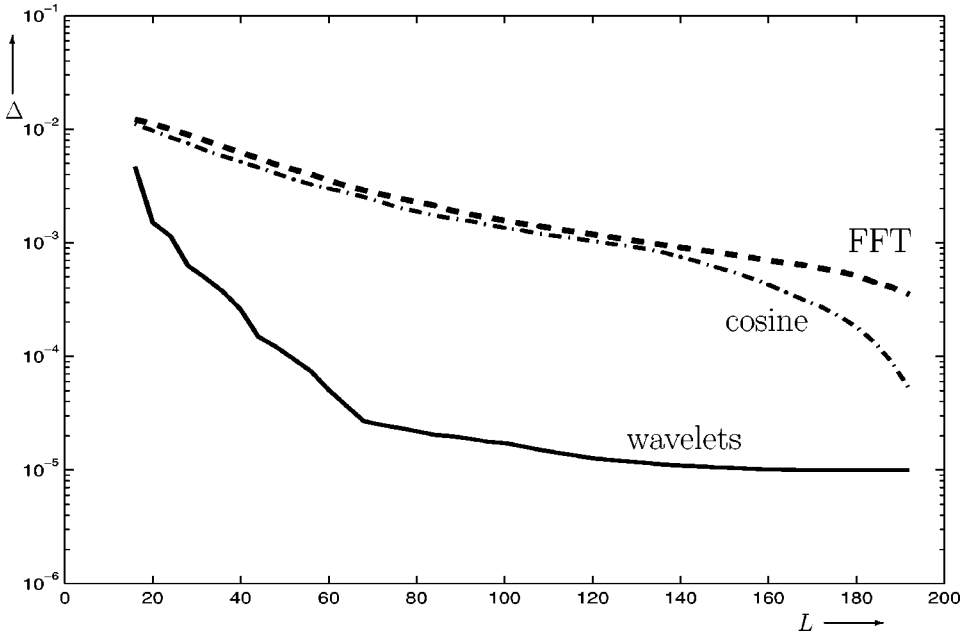

FIG. 7. Square-root error Δ between the rescaled TPCF of a homopolymer ring with $K=200$ and $|i-j|=100$ in the globular state and its approximations. The curves correspond to the wavelet approximation (solid line), FFT approximation (dashed line), and cosine approximation (dash-dotted line). The X axis is the number L of approximation coefficients used.

low reported errors are those from the fitting procedure only and do not necessarily account for statistical and other simulation errors.

We can see that the wavelet approximated functions agree with the most recent theoretical values much better. Note also that some of the theoretical values in this table have been updated thanks to the more accurate values from Refs. [3,23,32] as compared to those which we have used in Ref. [28]. Moreover, we do not even need to freeze δ at the theoretical value in order to extract a more accurate estimate for θ as we had to do previously. These improvements in the results of our fitting are not surprising given that, as we have mentioned earlier, the coefficient cut off leads to an effective noise suppressing.

The least-squares fitting of the data $\{\mathbf{x},\mathbf{y}\}$ with a model function $y(x_i;\mathbf{a})$, which depends on the fitting parameters $\mathbf{a}$ in a nonlinear fashion, in the multi variate case is a complex problem [34] akin to that of finding the global minimum of the merit function $\chi^2(\mathbf{a})=\Sigma_{i=1}^{N}\sigma_i^{-2}[y_i-y(x_i;\mathbf{a})]^2$ with respect to N parameters $\mathbf{a}$, where σ_i is the standard deviation (error) of the ith data point. If the data are fairly noisy, the problem of finding the global minimum of χ^2 becomes complicated as there are many low-lying local minima of this function and its constant value surfaces have a complicated topology. The Marquardt-Levenberg method is one of the most popular fitting algorithms which is an efficient hybrid of the inverse-Hessian (variable metric) and the steepest-descent (conjugated gradients) minimization algorithms for χ^2 [34]. Practically, the iterations need to be stopped after the values of χ^2 change less than the specified precision and, clearly, the resulting fitted values $\mathbf{a}_{fit}$ may depend on the choice of the initial values $\mathbf{a}_0$ if there are many local minima present, as well as on the weights σ. It is not uncommon to find the parameters wandering around near the global minimum in a flat valley of complicated topology if the input data were fairly noisy [34]. The wavelet treatment renders the initial poorly defined fitting problem into a well-defined one (which becomes essentially independent of the initial parameters choice) by removing the high-pitch statistical noise from the data and thus by simplifying the topology of the constant χ^2 surfaces and getting rid of its many artificial local minima. At the same time, the variances (squared standard errors) of the fitted parameters and the covariances between them become smaller than for the untreated data as we are now guaranteed to have found the true χ^2 global minimum.

TABLE I. Comparison of the exponents δ and θ between the results from the direct fitting of the Monte Carlo data with those from their wavelet approximations (subscript *ww*) and the theoretical results (subscript *theor*) for open and ring homopolymer coils with the degree of polymerization $K=200$. Fitted values have been obtained by a four-parametric fit via Eq. (7).

	δ	δ_{ww}	δ_{theor}	θ	θ_{ww}	θ_{theor}
0	2.11±0.07	2.36±0.02	2.428±0.001	0.36±0.02	0.276±0.005	0.271±0.002
1	2.23±0.04	2.36±0.02	…	0.56±0.01	0.51±0.01	~0.46
1'	2.42±0.04	2.39±0.02	…	0.45±0.01	0.462±0.003	0.459±0.003
1"	2.04±0.08	2.39±0.02	…	0.68±0.03	0.52±0.02	~0.46
2	2.39±0.07	2.40±0.02	…	0.81±0.02	0.80±0.01	0.80±0.01
Ring	2.46±0.07	2.40±0.02	…	0.79±0.006	0.815±0.005	0.80±0.01

TABLE II. Values of the exponents δ and θ for star homopolymers with $f=12$ arms and $(N-1)/f=50$ arm length in a good solvent. The following notations for the monomer pairs have been adopted: $a:n$, $b:m$, where a,b number arms and n, m number monomers within arms and 0 refers to the core monomer. Other notations are the same as in Table I.

	δ	δ_{ww}	θ	θ_{ww}	θ_{theor}
0, $a:m=25$	2.67±0.03	2.67±0.002	3.036±0.04	3.024±0.02	2.677
0, $a:m=50$	2.56±0.03	2.62±0.01	0.59±0.02	1.51±0.01	1.442
$a:n=25$, $a:m=50$	2.40±0.06	2.48±0.004	0.55±0.01	0.50±0.003	0.458
$a:n=50$, $b:m=50$	2.30±0.03	2.18±0.01	0.23±0.01	0.26±0.007	0.277

Table II lists similar exponents for star homopolymers with the number of arms $f=12$ in a good solvent. Here we have used the wavelet approximation with $L=30$ coefficients. We then have compared the results with those from the analytical renormalization group calculations in the so-called "cone" approximation for θ from Ref. [33]. This comparison has not been previously made in Ref. [28] or elsewhere so far, to the best of our knowledge. The agreement between the Monte Carlo and theoretical values seems quite reasonable despite the relatively short length of the arms and the limitations of the "cone" approximation. The latter produces the contact exponents only dependent on the functionalities f_i, f_j of the two monomers in question and not on any other parameters of the star—namely

$$\theta_{f_i,f_j} \simeq \frac{5}{36}\frac{1}{\sqrt{2}-1}[(f_i+f_j)^{3/2}-f_i^{3/2}-f_j^{3/2}]. \qquad (18)$$

As one can see, the quality of the wavelet approximation is rather good for the combined scheme, while the number of approximating coefficients is quite small.

In general, the accuracy of the wavelet approximations with a fixed number of reconstruction coefficients depends on the chosen basis set. So far, no exact "recipe" was given on which basis we have to use in a concrete case. Thus, we have checked our assumption about one of the dual bases "RB5-5" by an additional study. As we are especially interested in the quality of the scaling exponent calculations we have evaluated the scaling exponent for an open homopolymer coil with the use of different bases. These results are presented in Table III. We have used the wavelet approximations of the end-end TPCF's with the same number of coefficients. We chose for this comparison typical representatives of the main wavelet families: Coifman 2, Daubechies 4, Symlet 4, biorthogonal 5-5, and discrete Meyer wavelets [9].

We can see that the "reverse biorthogonal 5-5" basis set does the approximation better than the other bases. On the other hand, other bases, apart from the discrete Meyer's, also reveal good fitting results compared to the untreated TPCF. This means that our current scheme is just one of possible successful choices of the basis set. The situation with the discrete Meyer basis is easily explained by a too large support length of this basis $l=60$ as compared with $l=11$ for "RB5-5," which is known to lead to strong oversmoothing [9].

IV. CONCLUSION

Our present study indicates that the discrete wavelets provide a suitable and powerful instrument for approximating the intrachain two-point correlation functions of different homopolymers in dilute solutions. The wavelet technique allows us to extract the scaling properties from fairly noisy data more accurately and reliably than can be done by direct fitting. The wavelet treatment removes the high-pitch stochastic fluctuations (part of the "statistical noise") in the data, thereby producing a somewhat "coarse-grained" approximation of the data. This renders the ill-defined multivariate nonlinear fitting procedure of the untreated data into a well-defined uniquely convergent fitting procedure after the wavelet treatment of the data. Naturally, this also reduces the standard deviations of the fitted parameters. However, the wavelet treatment does not oversmooth the data by retaining the genuine oscillations as we clearly see in the case of the globule; nor does it produce any of the unpleasant artifacts of the truncated Fourier approximation.

We can see that the dual basis set performs particularly well for approximating TPCF's. This is related to the basis properties—namely, that the decomposition functions have a maximal number of vanishing moments with a finite support, whereas the reconstruction functions are as regular as possible with a given length of support. Moreover, the proposed scheme is rather flexible as it is based on the conventional FWT algorithm. One can choose the basis set and adjust the

TABLE III. Comparison of the exponents δ and θ between the theoretical results, different wavelet approximations (with names of the wavelet bases are given in the first column), and the untreated results from the direct fitting of Monte Carlo data for the end-end TPCF's of an open homopolymer coil with the degree of polymerization $K=200$.

	δ	θ
Theoretical	2.428±0.001	0.271±0.002
"RB5-5"	2.36±0.02	0.276±0.005
"BR5-5"	2.36±0.02	0.31±0.01
Daubechies 4	2.35±0.02	0.29±0.02
Symlet 4	2.34±0.02	0.28±0.02
Coifman 2	2.36±0.02	0.285±0.005
Discrete Meyer	2.1±0.01	0.4±0.01
Untreated	2.11±0.07	0.36±0.02

number of the coefficients easily for a particular problem. From the results in Table III we can also conclude that by using almost any reasonable basis it is possible to obtain an improvement in the fitting procedure.

It should be emphasized that the wavelet scheme is rather universal. The scheme of the wavelet approximation proposed here allows us to represent the correlation functions with a small number of approximating coefficients not only for the coil but also for globular state of the homopolymers. For instance, our procedure yields the relative accuracy of the approximation of order $(1/n)\Delta \sim 0.5 \times 10^{-3}$. Such accurate knowledge of TPCF's can be used for an input to the self-consistent calculations of the interchain distribution functions in the framework of the density functional methods [35–37] and others.

Due to a compact parametrization and a high accuracy of the approximation by wavelets, we hope that the wavelets can be applied not only for approximating the interchain distribution functions of polymers, but also in order to calculate these functions by the integral equation theory of polymers [38]. The success of the recent applications of wavelets to the theory of molecular solutes [4] has indicated that the method is capable of calculating the thermodynamic characteristics of solvation rather accurately.

We believe that further progress in this direction can also be of importance for novel theories for calculating the intrachain TPCF's of polymers directly from a force field. Some of us are presently working on the super-Gaussian self-consistent (SGSC) theory for a single macromolecule with any two-body Hamiltonian, in which a set of integro-differential equations is derived for $\hat{g}_{ij}(\hat{r})$ as well as for D_{ij}. In order to reduce the computational expenses in such calculations, having a compact and multiresolution accurate representation for $\hat{g}_{ij}(\hat{r})$ is essential.

Finally, due to the very general nature of the wavelet theory, we hope that wavelets can find other numerous applications for describing the spatial and temporal dependences of various observables in a number of fields of soft condensed matter theory which they have not hereto beneficially influenced.

ACKNOWLEDGMENTS

We would like to thank Professor L. Schäfer, Dr. C. von Ferber, Dr. H.-J. Flad, Dr. H. Luo, and Professor D. Kolb for interesting discussions. We acknowledge the support of the Centre for Synthesis and Chemical Biology, and some of us (M.F. and G.C.) also acknowledge the support of the Russian Foundation for Basic Research.

[1] J. des Cloizeaux and G. Jannink, *Polymers in Solution* (Oxford Science, Oxford, 1990).
[2] J.-P. Hansen and I. R. McDonald, *Theory of Simple Liquids*, 2nd ed. (Academic, London, 1986).
[3] L. Schäfer, *Excluded Volume Effects in Polymer Solutions as Explained by the Renormalisation Group* (Springer-Verlag, Berlin, 1999), Chap. 16; L. Schäfer, U. Lehr, and C. Kappeler, J. Phys. I **1**, 211 (1991).
[4] G. N. Chuev and M. V. Fedorov, J. Comput. Chem. **25**, 1369 (2004).
[5] G. N. Chuev and M. V. Fedorov, J. Chem. Phys. **120**, 1191 (2004).
[6] G. N. Chuev and M. V. Fedorov, Phys. Rev. E **68**, 027702 (2003).
[7] S. G. Mallat, *A Wavelet Tour of Signal Processing*, 2nd ed. (Academic, San Diego, 1999).
[8] Y. Meyer, *Wavelets: Algorithms and Applications* (SIAM, Philadelphia, 1993).
[9] I. Daubechies, *Ten Lectures on Wavelets*, CBMS/NSF Series in Applied Math. No. 61 (SIAM, Philadelphia, 1992).
[10] D. L. Donoho, Appl. Comput. Harmon. Anal. **1**, 100 (1993); D. L. Donoho, M. Vetterli, R. A. DeVore, and I. Daubechies, IEEE Trans. Inf. Theory **44**, 2435 (1998).
[11] R. T. Ogden, *Essential Wavelets for Statistical Applications and Data Analysis* (Birkhauser, Boston, 1997).
[12] K. Cho, T. A. Arias, J. D. Joannopoulos, and P. K. Lam, Phys. Rev. Lett. **71**, 1808 (1993).
[13] S. Wei and M. Y. Chou, Phys. Rev. Lett. **76**, 2650 (1996).
[14] S. Goedecker and O. V. Ivanov, Comput. Phys. **12**, 548 (1998).
[15] S. Goedecker, *Wavelets and Their Application for the Solution of Partial Differential Equations in Physics* (Presses Polytechniques et Universitaires Romandes, Lausanne, 1998).
[16] S. Han, K. Cho, and J. Ihm, Phys. Rev. B **60**, 1437 (1999).
[17] S. Goedecker and I. Ivanov, Phys. Rev. B **59**, 7270 (1999); I. M. Dremin, O. V. Ivanov, and V. A. Nechitailo, Phys. Usp. **44**(5), 447 (2001),
[18] J.-P. Antoine, Ph. Antoine, and B. Piraux, in *Wavelets in Physics*, edited by J. C. van den Berg (Cambridge University Press, Cambridge, England, 1999), p. 299.
[19] T. A. Arias, Rev. Mod. Phys. **71**, 267 (1999).
[20] H.-J. Flad, W. Hackbusch, D. Kolb, and R. Schneider, J. Chem. Phys. **116**, 9641 (2002).
[21] H. Luo, D. Kolb, H.-J. Flad, W. Hackbusch, and T. Koprucki, J. Chem. Phys. **117**, 3625 (2002).
[22] A. B. Romeo, C. Horellou, and J. Bergh, Mon. Not. R. Astron. Soc. **342**, 337 (2003); **354**, 1208 (2004).
[23] R. Guida and J. Zinn-Justin, J. Phys. A **31**, 8103 (1998).
[24] E. G. Timoshenko and Yu. A. Kuznetsov, Colloids Surf., A **190**, 135 (2001).
[25] Yu. A. Kuznetsov and E. G. Timoshenko, J. Chem. Phys. **111**, 3744 (1999).
[26] F. Ganazzoli, Yu. A. Kuznetsov, and E. G. Timoshenko, Macromol. Theory Simul. **10**, 325 (2001).
[27] *Computer Simulation of Liquids*, edited by M. P. Allen and D. J. Tildesley, (Clarendon, Oxford, 1987).
[28] E. G. Timoshenko, Yu. A. Kuznetsov, and R. Connoly, J. Chem. Phys. **116**, 3905 (2002).
[29] W. Sweldens, Appl. Comput. Harmon. Anal. **3**, 86 (1996).
[30] G. Belkyn, R. Coifman, and V. Rokhlin, Commun. Pure Appl.

Math. **44**, 141 (1991).
[31] S. L. Marpl Jr., *Digital Spectral Analysis with Applications* (Prentice-Hall, Englewood Cliffs, NJ, 1987).
[32] S. Carraciolo, M. S. Causo, and A. Pelisetto, J. Chem. Phys. **112**, 7693 (2000).
[33] C. von Ferber, A. Jusufi, M. Watzlawek, C. N. Likos, and H. Löwen, Phys. Rev. E **62**, 6949 (2002); C. von Ferber, Nucl. Phys. B **490**, 511 (1997).
[34] W. H. Press, S. A. Teukolsky, W. T. Vetterling, and B. P. Flannery, *Numerical Recipes in C* (Cambridge University Press, Cambridge, England, 1992).
[35] A. Yethiraj, J. Chem. Phys. **109**, 3269 (1998).
[36] N. Patra, and A. Yethiraj, J. Chem. Phys. **118**, 4702 (2003).
[37] M. B. Sweatman, J. Phys.: Condens. Matter **15**, 3875 (2003).
[38] K. S. Schweizer and J. G. Curro, Adv. Chem. Phys. **98**, 1 (1997); P. A. Monson and G. P. Morriss, *ibid.* **77**, 451 (1990).